# Volume Constancy during Stretching of Spider Silk

G. V. Guinea, J. Pérez-Rigueiro, G. R. Plaza, and M. Elices*

*Departamento de Ciencia de Materiales, Universidad Politécnica de Madrid, ETS de Ingenieros de Caminos, c/ Profesor Aranguren s/n, 28040 Madrid, Spain*

*Received February 15, 2006; Revised Manuscript Received March 23, 2006*

The characterization of silk properties requires a reliable measurement of stress−strain curves from tensile tests, which calls for a detailed analysis of what is considered the cross section of the sample and how it varies during the experiments. Here, spider silk fibers from the major ampullate gland (MAS) of *Argiope trifasciata* spiders are tensile tested, and the cross-sectional area is measured under different strained configurations. It has been found that the fiber volume remains practically constant during stretching, and deformation proceeds homogeneously in all the fibers. The conservation of volume is validated independently of the type of fiber and the strain level. This result, applied to compute true stress−strain curves for different MAS fibers, shows that the description of their properties depends noticeably on which set of tensile parameters is chosen (true or engineering), and that engineering values could lead to misinterpretation of experiments that combine results from different strain ranges.

## 1. Introduction

Spider silks spun by orb-weaving spiders have evolved to absorb and dissipate mechanical energy in structures that require a minimum amount of material.[1,2] This ability depends on a combination of tensile properties rarely found in other materials: spider silk combines a tensile strength comparable to that of high-performance fibers[3] with a large deformation at breaking. The interest in mimicking these properties is driving an increasing effort to understand the basis of this behavior and to reproduce it in artificial fibers inspired by spider silk.[4]

However, the peculiarities of spider silk have contributed toward making the analysis of its microstructure and properties an elusive task. For instance, the reliable characterization of its mechanical behavior in a tensile test, which is considered a routine technique for most materials, has required considerable effort for several decades. The small cross-sectional area of the fiber complicates the rescaling of force into stress, and consequently, initial works presented the results of tensile tests as force vs displacement curves,[5,6] which prevented a precise comparison of the properties of silk and those of other materials. The reliable calculation of stress−strain curves from tensile tests became a standard procedure with the use of scanning electron microscopy to measure the diameter of the fibers.[7,8]

Rescaling force and displacement into stress and strain requires careful consideration of what is considered the cross section of the sample. The most obvious choice is to use the initial cross-sectional area, $A_0$, and initial length, $L_0$, of the sample, so that stress and strain (labeled *engineering* stress, *s*, and *engineering* strain, *e*) are defined as

$$s = \frac{F}{A_0} \quad e = \frac{L - L_0}{L_0} = \frac{L}{L_0} - 1 \tag{1}$$

with *F* being the applied force and *L* the length of the sample.

An alternative definition appears if stress and strain are referred to the instantaneous values of cross-sectional area, *A*, and length, *L*. Stress and strain defined in this way are labeled *true* stress, $\sigma$, and *true* strain, $\epsilon$.

$$\sigma = \frac{F}{A} \quad \mathrm{d}\epsilon = \frac{\mathrm{d}L}{L} \tag{2}$$

The conversion of engineering strain into true strain is simply given by the expression

$$\epsilon = \ln\left(\frac{L}{L_0}\right) = \ln(1 + e) \tag{3}$$

In contrast, the conversion of engineering stress into true stress requires a determination of the changes of the cross-sectional area during the tensile test. A usual hypothesis assumes that the volume remains constant during the tensile test

$$A_0 L_0 = AL \tag{4}$$

In this case, true and engineering stresses are related by the expression

$$\sigma = s\,\frac{L}{L_0} \tag{5}$$

As seen from eq 5, the hypothesis of constant volume yields a simple relationship between engineering and true stresses. It should be noted, however, that the conservation of volume during tensile testing is not a general law valid for any material—actually, it is not applicable in most of them—and requires careful checking in each case.

A distinction between engineering and true magnitudes is not relevant in the range of small deformations, since $\mathrm{d}\epsilon = \mathrm{d}e/(1 + e) \approx \mathrm{d}e$, but the two sets of magnitudes may differ appreciably in the range of large deformations. Since the excellent mechanical behavior of spider silk is the result of its ability to sustain large deformations, the description of the tensile properties of spider silk will depend on which set of parameters is chosen.

Besides, it has been found that changes in the initial length of the fibers either by supercontraction (a reduction of the initial length of spider silk fibers when submerged in water with the ends unrestrained[9]) or stretching[10] induce large changes in the tensile properties of silk, especially in the stresses and strains at breaking. Figure 1 shows that the tensile behavior of spider silk ranges from the stiff fibers retrieved by forced silking (FS) to the extremely compliant fibers after supercontraction (maxi-

* To whom all correspondence should be addressed. Tel. +34913366754; Fax +34913366680; e-mail: melices@mater.upm.es.

10.1021/bm060138v CCC: $33.50 
Published on Web 05/28/2006

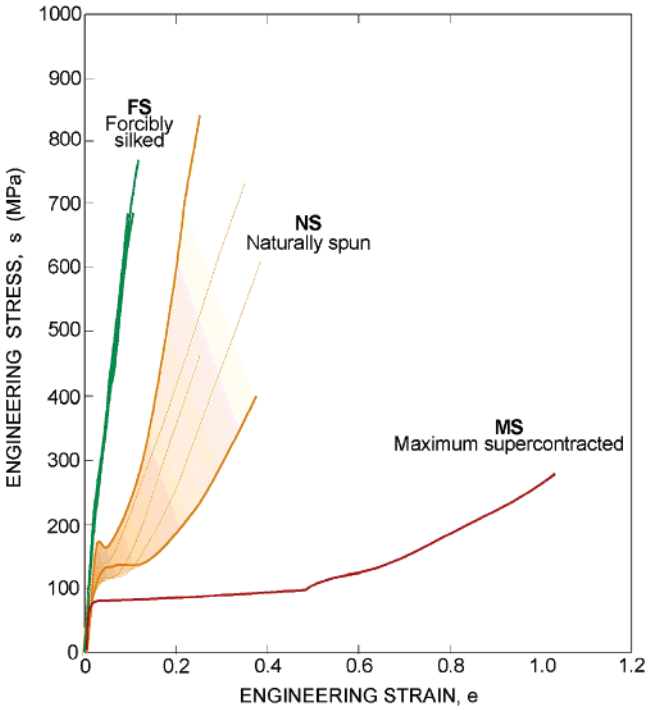


**Figure 1.** Engineering stress−strain curves of major ampullate gland silk (MAS) from *A. trifasciata*. FS: forcibly silked fibers. NS: naturally spun fibers, i.e., fibers retrieved either from the web or from the safety line. MS: maximum supercontracted fibers, i.e., fibers subjected to supercontraction and subsequent drying. All tests were performed at 20 °C, 35% RH, and strain rate 0.0002 $s^{-1}$.

mum supercontracted fibers, MS), including the whole range of tensile properties displayed by fibers naturally spun (NS) by the spider either in the web or as a safety line. An adequate comparison of tensile curves has to account for changes in fiber geometry during stretching, and consequently, it would be very convenient either to prove the hypothesis of constant volume for spider silk or find a relationship between the initial cross-sectional area and the instantaneous cross-sectional area during tensile testing.

Unfortunately, testing the hypothesis of constant volume in spider silk has proven a difficult task, mainly due to the low reproducibility of silk fibers. The large variability observed in spider silk fibers is thought to endow the spider with the ability of adapting its properties to its immediate requirements,[11] but this has been a major drawback in the experimental study of spider silk.[12] The large scattering observed in control samples does not allow one to draw any firm conclusion from testing fibers under different conditions of interest. As to the hypothesis of constant volume, the large variability of the diameter of control samples allows no observation of a clear trend when analyzing the diameters of fibers subjected to different degrees of stretching.

Despite this drawback, the hypothesis of constant volume has been applied to spider silk mainly on account of its simplicity,[13] and it has been shown to yield consistent results even under combined processes of stretching and controlled supercontraction.[10] However, most studies of the tensile properties of spider silk are conventionally presented in terms of engineering magnitudes,[11,14] in part because the validity of the hypothesis of constant volume does not rest on a sound experimental basis.

In this study, spider silk fibers of reproducible properties were retrieved in sufficient quantities by applying the initial observation of Work[9] that adjacent samples show comparable tensile properties, and also with some advances in the methodology of forced silking developed by the authors.[15,16] Silk samples were tensile tested, and the cross-sectional area measured under different strained configurations and compared with that of control samples. It was found that the hypothesis of constant volume applies with good accuracy. This was used to recalculate the true stress−true strain curves of spider silk samples, so that the tensile properties of forcibly silked (FS), maximum supercontracted (MS), and naturally spun (NS) fibers could be compared consistently.

**Table 1.** Mean Silking Stresses of the Four Silking Processes and Diameters (mean ± standard error) as Calculated from the Control Samples

| silking process | number of control samples | silking stress (MPa) | diameter (mean ± s.e.) |
|---|---|---|---|
| 1 | 3 | 290 | 4.5 ± 0.1 |
| 2 | 6 | 274 | 2.8 ± 0.1 |
| 3 | 19 | 148 | 3.3 ± 0.1 |
| 4 | 10 | 25 | 3.1 ± 0.1 |

## 2. Experimental Methods

*Argiope trifasciata* spiders have been used as a source of major ampullate gland (MAS) silk. *A. trifasciata* is a Mediterranean spider whose size allows easy manipulation. MAS silk was obtained by forced silking.[17] The details of the silking procedure are given elsewhere.[15] Briefly, the spider is immobilized in a self-zipping bag, in which a hole has been perforated to make the spinneret accessible. Silk samples were retrieved from four different monitored silking processes,[16] so that the silking force of each process could be measured. The measurement of the diameter of the fibers allowed the calculation of silking stress and the sorting of them according to their tensile properties. Following this rationale, the silking processes presented in this work were chosen to span the whole range of properties from NS to FS fibers. The silking stresses of the four processes are indicated in Table 1. Forced silking processes proceeded at 20 mm/s.

The silk samples (25 mm gauge length) were secured on perforated aluminum foil frames.[18] Adjacent samples were used to ensure the reproducibility of the results. One out of two samples was chosen as a control, and its diameter was measured.[9] At least five sections of each fiber were analyzed, so that a micrograph was taken every 5 mm along the sample, as illustrated in Figure 2. The mean diameter and the standard error of the control samples measured from every silking process are shown in Table 1. From these data, it is apparent that the diameter of the fiber remains almost constant along its whole length. The diameter of any tested sample was compared with the mean value of the diameters of the adjacent control samples. The precision of the measurements from SEM micrographs has been determined from the size of a pixel as 0.03 $\mu$m.

Tensile tests were performed in an Instron 3309−662/8501 tensile testing machine appended to an environmental chamber (Dycometal CCK-25/300). Forces were measured by a 100 mN load cell with 0.1 mN resolution (HBM 1-Q11). The tests were performed at 20 °C and 35% relative humidity at a loading speed of 1 mm/min.

In each case, the tensile test was stopped on reaching a predetermined strain. The ends of the silk sample were glued on a stiff plastic tape prior to unloading, so that the strain was maintained during further manipulation. Then, the fiber was removed from the testing machine. The range of strains for each class of fibers was chosen to include information of the conservation of volume for strains before the yield point ($e = 0.02$) and to ensure that a negligible number of fibers could break during testing ($e = 0.15$; $\sigma \approx 600$ MPa).

The samples were sputtered with gold (distance from the sample to the cathode 50 mm, sputtering time 5 min) and examined in a JEOL 6300 scanning electron microscope (observation conditions $V = 10$ kV; $I = 0.06$ nA). At least four micrographs were taken of each sample, and two diameters were measured from each micrograph. Diameters

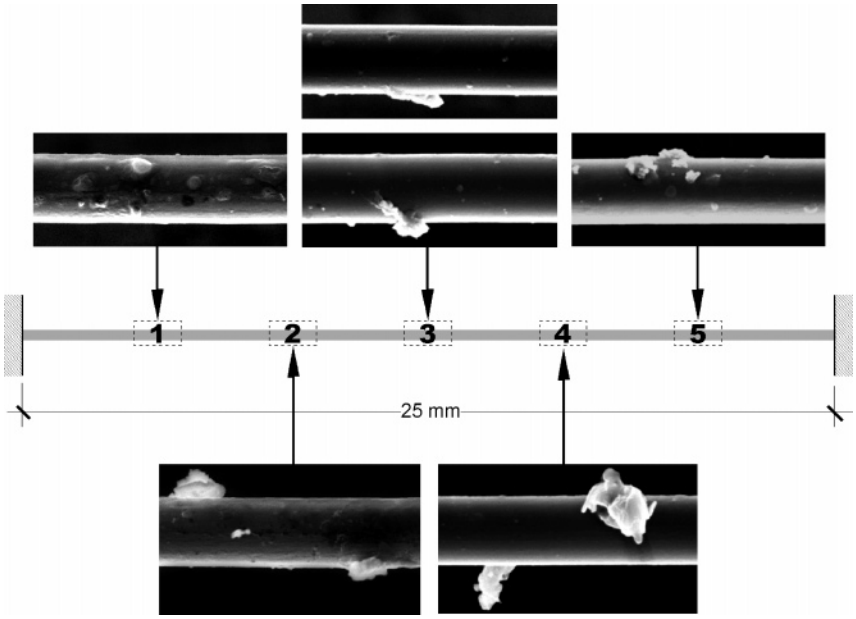


**Figure 2.** Illustration of the distribution of micrographs taken along a silk sample to measure its diameter. The two micrographs of region 3 correspond to rotating the fiber 50° around its long axis.[19] The length of each micrograph is 17.2 $\mu$m.

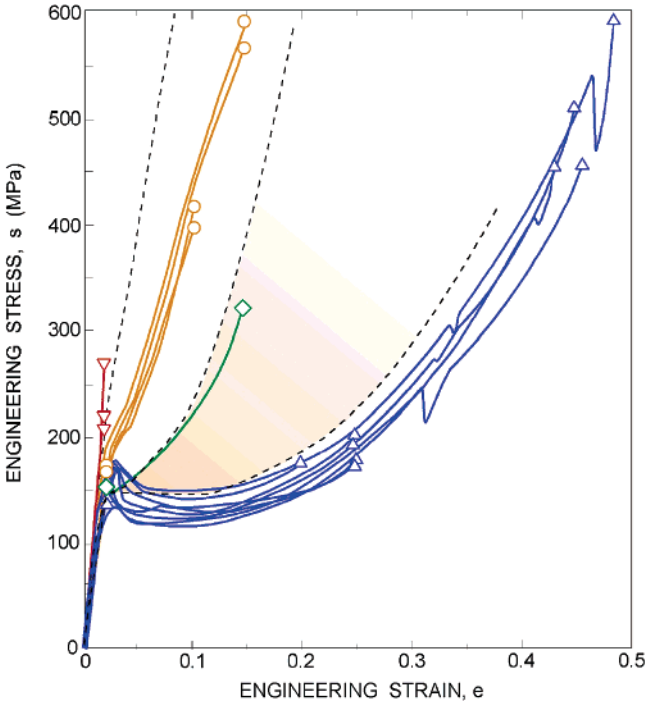


**Figure 3.** Engineering stress−strain curves for the four groups of fibers used in this study. Symbols indicate the points at which tests were stopped. All tests were performed at 20 °C, 35% RH, and strain rate 0.0002 $s^{-1}$. FS and NS ranges from Figure 1 are also shown as references.

measured from micrographs of the same section of the fiber taken at two different orientations differed at most by 5%.[19] Consequently, the mean value of the diameters was used to calculate the cross-sectional area of the fiber, assuming a circular cross section.[19]

## 3. Results and Discussion

Figure 3 plots the engineering stress−strain curves considered in this work. The points at which the tensile tests were stopped are marked with open symbols. To serve as a reference, this figure also shows the typical range of FS and NS fibers. A total of 27 tests were performed at 6 different engineering strain levels, ranging from 0.02 to 0.45.

Tensile curves in Figure 3 show different types of behavior, from stiff—typical of most FS fibers—to compliant ones, spanning the whole range of natural fibers, though all of the fibers were obtained by the forced silking procedure described in the section above. The possibility of obtaining different kinds of fiber by forced silking—even resembling natural ones—was demonstrated in previous papers by the authors.[16,20] In this work, four silking processes with different *spinning stresses* were considered, aiming at obtaining silk fibers with different tensile properties. The color code and markers in Figure 3 identify fibers from the same silking process.

Strained fibers were metallized and observed by scanning electron microscopy to measure their diameter. All the samples showed homogeneous deformation regardless of the strain they were subjected to. The strained volume, $V$, was then computed as the product of the actual fiber length, $L$, times the actual cross section, $A$, calculated from the diameter measured on the strained fiber

$$V = AL \tag{6}$$

To deduce the initial volume, both the initial fiber length, $L_0$, and the initial cross-sectional area, $A_0$, were considered

$$V_0 = A_0 L_0 \tag{7}$$

The initial area $A_0$ was obtained from the averaged diameter, $\phi_0$, of the two control samples adjacent to both ends of the fiber tested. The volume ratio was calculated as

$$V/V_0 = (A/A_0)(L/L_0) = (\phi/\phi_0)^2(1 + e) \tag{8}$$

with $\phi$ being the fiber diameter at the engineering strain $e$.

Figure 4 shows the plot of $V/V_0$ as a function of the engineering strain $e$. Each point corresponds to the $V/V_0$ ratio of 1 of the 27 fibers tested in this work. Different symbols are used for points of the same silking process, in accordance with Figure 3. Although some scatter appears, all the experimental points lie around the horizontal line that indicates the volume constancy condition $V = V_0$. Table 2 shows the values of $V/V_0$

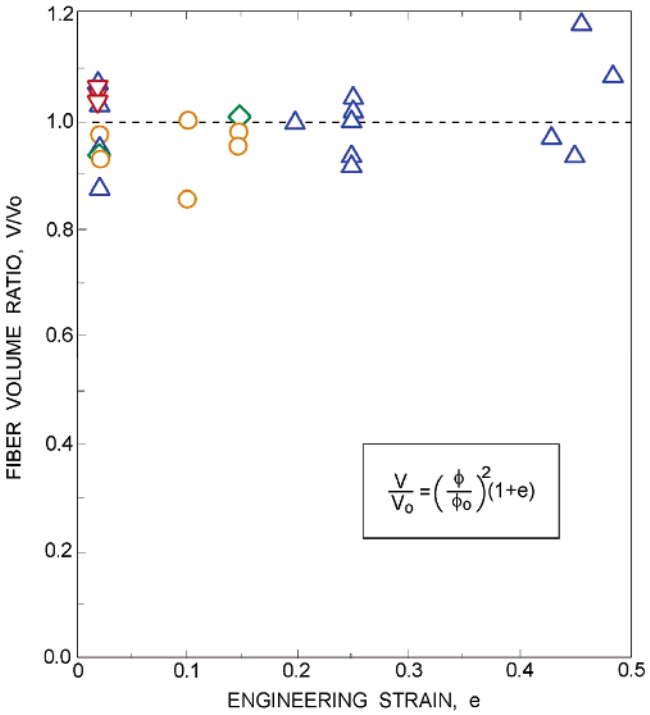


**Figure 4.** Ratio between the volume of strained fibers and the initial volume as a function of engineering strain in the fibers shown in Figure 3.

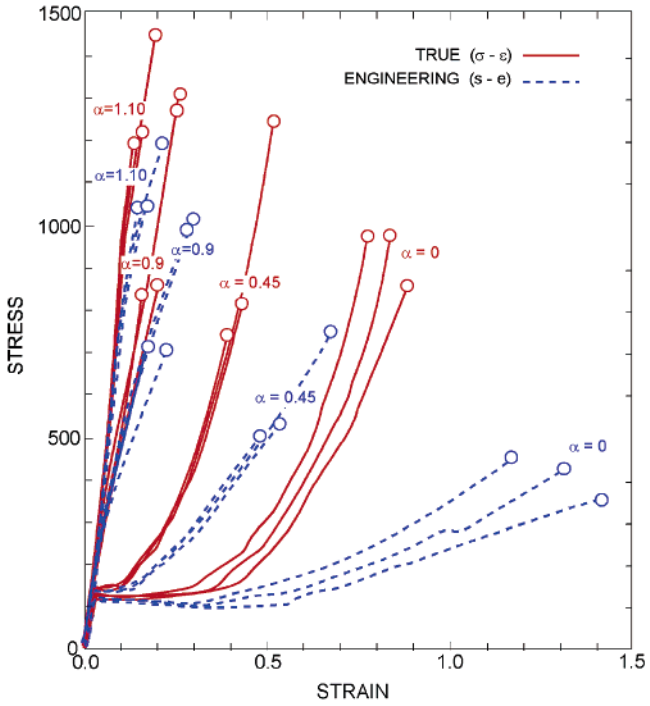


**Figure 5.** Engineering (dashed lines) and true stress−strain (solid lines) curves for silk fibers with different alignment parameters α (defined in the text). Symbols indicate the points of rupture. All tests were performed at 20 °C, 35% RH, and strain rate 0.0002 $s^{-1}$.

as a function of strain level, grouped according to the silking process. The mean value and standard error of all the measurements is 0.993 ± 0.013, so the stretching of silk fibers can be considered to proceed at constant volume.

The effect of the type of fiber tested—whether stiff or compliant—seems to be irrelevant to volume constancy, as deduced from Figure 4 and Table 2, and this is true also of the strain level (from 0.02 to 0.45), since individual and aggregated values for different silking processes and at different strain levels are comparable within the experimental scatter.

Since all the types of fiber in Figure 3 share the same protein composition, the differences in stress−strain curves are the result of changes in processing, which results in different degrees of molecular alignment.[21−24] Consequently, strain levels are not biunivocally associated with a particular molecular conformation in all the samples: the same strain level can correspond in one fiber to the plateau region (usually associated with a strong disoriented and coiled molecular structure[25,26]), whereas in another fiber, this strain is placed in the hardening region (where molecules are being reoriented under the stretching stress).

Despite the experimental scatter, the data in Figure 4 and Table 2 suggest that with a good approximation the volume of silk fibers remains constant throughout the stretching process, independently of the degree of alignment and the molecular configuration reached by the fiber. This hypothesis is supported by experimental data on crystal orientation of forcibly silked *Nephila clavipes* silk fibers, which is consistent with affine deformation at constant volume up to fiber rupture at ~10% strain.[21] Within this framework, the tensile behavior of silk would correspond to that of an elastomeric material whose properties are controlled by a double network of hydrogen bonds and protein chains.[27]

By extension, the increment of volume beyond yielding observed in several polymers under tensile testing has been commonly associated with the presence of crazing and other irreversible damage processes[28−30] that have not been observed in spider silk fibers. In this context, the volume constancy observed in spider silk agrees well with the fact that permanent deformation of these fibers is fully reversible, with the possibility to recover the properties of silk fibers once strained, as was demonstrated by the authors in a previous work.[10] The chains in the amorphous fraction extend during a tensile test in air, breaking hydrogen bonds and developing new ones, but these conformational changes are reversible if the hydrogen bond network is "melted" by increasing humidity, and the fiber is not completely restrained.

An interesting consequence of volume constancy upon stretching is the possibility of calculating true stresses by means of eq 5, without resort to a continuous measurement of fiber diameter throughout the test.

Figure 5 shows the stress−strain curves of silk fibers classified according to their degree of molecular orientation, measured through the *alignment parameter* α. The alignment

**Table 2.** $V/V_0$ Values (mean ± standard error) of Four Silking Processes at Different Strain Levels

| silking process | $e = 0.02$ | $e = 0.10$ | $e = 0.15$ | $e = 0.20$ | $e = 0.25$ | $e = 0.45$ | mean |
|---|---|---|---|---|---|---|---|
| 1 | 1.030 | | | | | | 1.030 ± 0.008 |
| 2 | 0.946 | 0.924 | 0.965 | | | | 0.945 ± 0.021 |
| 3 | 0.932 | | 1.009 | | | | 0.970 ± 0.038 |
| 4 | 0.981 | | | 1.008 | 0.993 | 1.051 | 1.006 ± 0.020 |
| mean | 0.988 ± 0.017 | 0.924 ± 0.075 | 0.980 ± 0.016 | 1.008 | 0.993 ± 0.025 | 1.051± 0.056 | 0.993 ± 0.013 |

**Table 3.** True ($\sigma_u$) and Engineering ($s_u$) Breaking Strength (mean ± standard error) of Fibers with Four Different Alignment Parameters[a]

| alignment parameter, α | $s_u$ (MPa) | | $\sigma_u$ (MPa) | |
|---|---|---|---|---|
| 0 | 407 ± 28 | $P = 0.0003$ | 932 ± 40 | $P = 0.0200$ |
| 0.45 | 589 ± 78 | | 930 ± 160 | |
| 0.90 | 853 ± 85 | | 1066 ± 128 | |
| 1.10 | 1090 ± 51 | | 1281 ± 82 | |
| mean | 744 ± 79 | | 1053 ± 64 | |

[a] Unpaired student's *T* probability level is given for the two extremes.

parameter is defined as $\alpha = L_0/L_{SC} - 1$, where $L_0$ is the initial length of the fiber and $L_{SC}$ the length when it is supercontracted.[24]

Four sets of curves are shown in Figure 5, with α equal to 0, 0.45, 0.90, and 1.10. A value of zero for the alignment parameter corresponds to supercontracted fibers (MS), that represent the lowest limit of the tensile properties. Fibers with $\alpha = 0.45$ behave like compliant NS fibers (see Figure 1). Alignment parameters above 0.9 yield fibers with stress−strain curves similar to those of forcibly silked fibers (FS).

As deduced from Figure 5, the use of true stress−strain curves does not change the deformational trends observed in engineering variables, since stiffness increases monotonically, as expected, with the alignment parameter in both sets of variables.

Even so, despite the experimental scatter, the interpretation of breaking stress values can be rather biased if only engineering stresses are considered, as is shown in Table 3. The engineering values in this table suggest that the stress at breaking diminishes as the fiber becomes more compliant. MS fibers show the lowest engineering breaking strength, while FS fibers show the highest. In addition, when unpaired Student's *T* test is applied to see whether the two extreme groups $\alpha = 0$ and $\alpha = 1.1$ are really different (i.e., to know the probability of obtaining by chance the measured engineering breaking strengths assuming that the two groups are drawn from a single population) a probability level of $P = 0.0003$ is obtained. This very low *P*-value is routinely interpreted in statistical terms as "extremely significant", and the logical conclusion is that the two groups are different and that fiber alignment has a definite effect on tensile strength. On the contrary, when true stresses are considered, the differences between groups are less evident, and the probability of obtaining both sets of data from a single population increases by almost 2 orders of magnitude ($P = 0.02$).

## 4. Conclusions

The conservation of volume during the tensile testing of spider silk fibers is validated experimentally in this work. Twenty-seven fibers with various degrees of alignments, from stiff FS-type to compliant NS, were tensile tested at up to six different engineering strain levels (*e* values ranging from 0.02 to 0.45). The diameters of the strained samples were measured by scanning electron microscopy, which confirmed the presence of a homogeneous state of deformation in all the fibers. Fiber volume, computed with the assumption of a circular cross section, remains practically constant during stretching, with a mean value slightly under unity. The type of fiber and the strain level seem to have little significant effect on the volumetric strain, within the experimental scatter.

These observations are in agreement with indirect findings by other authors, which have shown that the molecular orientation of FS spider fibers determined by nuclear magnetic resonance can be suitably explained if deformation proceeds at constant volume.[21]

The hypothesis of constant volume is applied to the rescaling of tensile tests of four groups of fibers with different degree of alignment, from MS to FS, to show that the distinction between engineering and true stresses is important when large deformations are involved, typically over $e = 0.30$. The description of the tensile properties of spider silk depend on which set of parameters is chosen, since engineering values could lead to a misinterpretation of experiments that combine results from different strain ranges.

**Acknowledgment.** The authors wish to thank José Miguel Martínez for his help with drawing figures. The spiders used in this study were kindly provided by Jesús Miñano (Universidad de Murcia, Spain) and reared by Oscar Campos and Iván Blanco (Naturaleza Misteriosa, Parque Zoológico de Madrid, Spain). This work was funded by Ministerio de Ciencia y Tecnología (Spain) through projects MAT 2003-04906 and by Comunidad de Madrid through project GR/MAT/0038/2004.

## References and Notes

(1) Kaplan, D. L.; Lombardi, S. J.; Muller, W. S.; Fossey, S. A. In *Biomaterials. Novel Materials from Biological Sources*; Byrom, D., Ed.; Stockton Press: New York, 1991; p 1.
(2) Elices, M., Ed. *Structural Biological Materials*; Pergamon Press: Amsterdam, 2000.
(3) Elices, M., Llorca, J., Eds. *Fiber Fracture*; Elsevier: Amsterdam, 2002.
(4) Lazaris, A.; Arcidiacono, S.; Huang, Y.; Zhou, J.-F.; Duguay, F.; Chretien, N.; Welsh, E. A.; Soares, J. W.; Karatzas, C. N. *Science* **2002**, *295*, 472.
(5) Lucas, F.; Shaw, J. T. B.; Smith, S. G. *J. Textile Inst.* **1955**, *46*, 440.
(6) Lucas, F. *Discovery*, January, 1964, p 20.
(7) Work, R. W. *Text. Res. J.* July, 1976, p 485.
(8) Denny, M. *J. Exp. Biol.* **1976**, *65*, 483.
(9) Work, R. W. *Textile Res. J.* **1977**, *47*, 650.
(10) Elices, M.; Pérez-Rigueiro, J.; Plaza, G.; Guinea, G. V. *J. Appl. Polym. Sci.* **2004**, *92*, 3537.
(11) Madsen, B.; Shao, Z. Z.; Vollrath, F. *Int. J. Biol. Macromol.* **1999**, *24*, 301.
(12) Dunaway, D. L.; Thiel, B. L.; Viney, C. *J. Appl. Polym. Sci.* **1995**, *58*, 675.
(13) Griffiths, J. R.; Salinatri, V. R. *J. Mater. Sci.* **1980**, *15*, 491.
(14) Garrido, M. A.; Elices, M.; Viney, C.; Pérez-Rigueiro, J. *Polymer* **2002**, *43*, 1537.
(15) Guinea, G. V.; Elices, M.; Real, J. I.; Gutiérrez, S.; Pérez-Rigueiro, J. *J. Exp. Zool.* **2005**, *303A*, 37.
(16) Pérez-Rigueiro, J.; Elices, M.; Plaza, G.; Real, J. I.; Guinea, G. V. *J. Exp. Biol.* **2005**, *208*, 2633.
(17) Work, R. W.; Emerson, P. D. *J. Arachnol.* **1982**, *10*, 1.
(18) Guinea, G. V.; Elices, M.; Pérez-Rigueiro, J.; Plaza, G. *Polymer* **2003**, *44*, 5785.
(19) Pérez-Rigueiro, J.; Elices, M.; Llorca, J.; Viney, C. *J. Appl. Polym. Sci.* **2001**, *82*, 2245.
(20) Pérez-Rigueiro, J.; Elices, M.; Plaza, G.; Real, J. I.; Guinea G. V. *J. Exp. Biol.* **2006**, *209*, 320.
(21) Grubb. D. T.; Jelinski, L. W. *Macromolecules* **1997**, *30*, 2860.
(22) Grubb, D. T.; Ji, G. *Int. J. Biol. Macromol.* **1999**, *24*, 203.
(23) Pérez-Rigueiro, J.; Elices, M.; Guinea, G. V. *Polymer* **2003**, *44*, 3733.
(24) Guinea, G. V.; Elices, M.; Pérez-Rigueiro, J.; Plaza, G. R. *J. Exp. Biol.* **2005**, *208*, 25.
(25) Shao, Z.; Young, R. J.; Vollrath, F. *Int. J. Biol. Macromol.* **1999**, *24*, 295.
(26) Eles, P. T.; Michal, C. A. *Macromolecules* **2004**, *37*, 1342.
(27) Termonia, Y. In *Structural Biological Materials*; Elices, M., Ed.; Pergamon Press: Amsterdam, 2000; p 335.
(28) Rezgui, F.; Swistek, M.; Hiver, J. M.; G'Sell, C.; Sadoun, T. *Polymer* **2005**, *46*, 7370−7385.
(29) Bai, S. L.; G'Sell, C.; Hiver, J. M.; Mathieu, C. *Polymer* **2005**, *46*, 6437.
(30) G'Sell, C.; Hiver, J. M.; Dahoun, A. *Int. J. Solids Struct.* **2002**, *39*, 3857.

BM060138V